

Relationship of Iron Deposition to Calcium Deposition in Human Aortic Valve Leaflets



Marion Morvan, BS,^{a,*} Dimitri Arangalage, MD, PhD,^{a,b,c,*} Grégory Franck, PhD,^{a,*} Fanny Perez, MD,^a Léa Cattan-Levy, MD,^{a,b} Isabelle Codogno, BS,^b Marie-Paule Jacob-Lenet, PhD,^a Catherine Deschildre, BS,^a Christine Choqueux, BS,^a Guillaume Even, BS,^a Jean-Baptiste Michel, MD, PhD,^a Magnus Bäck, MD, PhD,^d David Messika-Zeitoun, MD, PhD,^{a,b,c} Antonino Nicoletti, PhD,^{a,c} Giuseppina Caligiuri, MD, PhD,^{a,b,†} Jamila Laschet, PhD^{a,c,†}

ABSTRACT

BACKGROUND Intraleaflet hematomas are associated with advanced stages of aortic valve calcification and suspected to be involved in disease progression. However, the mechanism by which the entry of blood cells into the valves affects the biology of aortic valvular interstitial cells (VICs) remains to be elucidated.

OBJECTIVES This study sought to evaluate the putative link between intraleaflet hematoma and aortic valve calcification and to assess its pathophysiological implications.

METHODS The spatial relationship between calcium deposits and intraleaflet hematomas was analyzed by whole-mount staining of calcified and noncalcified human aortic valves, obtained in the context of heart transplantation and from patients who underwent surgical valve replacement. Endothelial microfissuring was evaluated by en face immunofluorescence and scanning electron microscopic analyses of the fibrosa surface. Red blood cell (RBC) preparations were used in vitro to assess, by immunofluorescence microscopy and Alizarin red staining, the potential impact of intraleaflet hematomas on phenotypic changes in VICs.

RESULTS Intraleaflet hematomas, revealed by iron deposits and RBCs into the fibrosa, secondary to endothelial microfissuring, were consistently found in noncalcified valves. The contact of primary VICs derived from these valves with RBCs resulted in a global inflammatory and osteoblastic phenotype, reflected by the up-regulation of interleukin-6, interleukin-1 β , bone sialoprotein, osteoprotegerin, receptor activator of nuclear factor kappa B, bone morphogenic protein 2, and muscle segment homeobox 2, the production of osteocalcin, and the formation of calcium deposits.

CONCLUSIONS The acquisition of an osteoblastic phenotype in VICs that come into contact with the senescent RBCs of intraleaflet hematomas may play a critical role in the initiation of calcium deposition into the fibrosa of human aortic valves. (J Am Coll Cardiol 2019;73:1043–54) © 2019 by the American College of Cardiology Foundation.



Listen to this manuscript's audio summary by Editor-in-Chief Dr. Valentin Fuster on JACC.org.

From the ^aNational Institute of Health and Medical Research U1148, Paris, France; ^bDepartment of Cardiology, Bichat Hospital, Paris, France; ^cFaculty of Medicine Paris-Diderot, University Paris Diderot, Sorbonne Paris Cité, Paris, France; and the ^dDepartment of Cardiology, Karolinska University Hospital, Stockholm, Sweden. *Drs. Morvan, Arangalage, and Franck are joint first authors and contributed equally to this work. †Drs. Caligiuri and Laschet are joint senior authors and contributed equally to this work. This work was supported by the Fondation de France (FDF 2013 00038582) and by the French Government through the National Research Agency (ANR) Program Investissements d'Avenir (ANR-16-RHUS-0003_STOP-AS, and ANR16-RHUS-00010_iVASC). The GENERAC study was supported by grants from the Assistance Publique-Hôpitaux de Paris (PHRC National 2005 and 2010 and PHRC regional 2007). Dr. Franck has received research grants from the Fondation Lefoulon-Delalande and the European Union PRESTIGE program (2017-1-0032). Drs. Perez and Cattan-Levy have received grants from the Fédération Française de Cardiologie (FFC). All other authors have reported that they have no relationships relevant to the contents of this paper to disclose.

Manuscript received June 18, 2018; revised manuscript received November 8, 2018, accepted December 2, 2018.

ABBREVIATIONS AND ACRONYMS

AC = aortic valve calcification

AS = aortic valve stenosis

f-RBC = fresh red blood cell

IL = interleukin

PBS = phosphate-buffered saline

PFA = paraformaldehyde

RBC = red blood cell

s-RBC = senescent red blood cell

VEC = valvular endothelial cell

VIC = valvular interstitial cell

Stenosis secondary to degenerative aortic valve calcification (AC) is the most frequent valvular heart disease in the Western world, and its prevalence, along with its public health burden, is increasing (1,2). Although several mechanisms and pathways involved in the progression of AC have been described (3-5), little is known about the nature of the endogenous stimuli that initiate and trigger the cascade leading to the calcification of aortic valve leaflets. In nonpathological conditions, aortic valve leaflets are avascular and fully covered by valvular endothelial cells (VECs) that protect the valvular interstitial cells (VICs),

nested in deeper layers of the fibrosa, from the bloodstream and its components. Past studies have linked intraleaflet hemorrhage, supposedly originating from neovascularization in human degenerative aortic valve stenosis (AS), to a more rapid progression of AC (6,7). Whether intraleaflet hemorrhages are a cause or a result of calcium deposition cannot be inferred from these studies because they were exclusively conducted on severely calcified valves at advanced stages of the disease. In addition, establishing the spatial relationship between calcium deposition and post-hemorrhagic hematomas requires an analysis of the whole valve structure, not merely the sections of valve leaflets as performed thus far.

SEE PAGE 1055

In the present study, we established a novel whole-mount immunohistological method and used it to analyze human aortic valves taken at the earliest stages of calcification. We hypothesized that a weakened endothelial barrier exposed to extreme hemodynamic conditions could contribute to the formation of intraleaflet hematomas and that the subsequent contact between VICs and the infiltrated, rapidly senescent red blood cells (RBCs) could represent an initial step toward valve vulnerability by promoting calcification within VICs.

METHODS

AORTIC VALVE COLLECTION. Aortic valves were collected (Biobank BRIF: BB-0033-00029) from: 1) consecutive patients who underwent surgical aortic valve replacement for severe AS and who were enrolled in an ongoing prospective cohort, GENERAC (Genetic of Aortic Valve Stenosis-Clinical and Therapeutic Implications) (NCT00647088), which is aiming to identify factors involved in AS occurrence and progression; 2) patients who underwent combined

coronary bypass grafting and aortic valve replacement for moderate AS; 3) patients with healthy, calcium-free aortic valve leaflets who underwent aortic valve replacement for severe pure aortic regurgitation not related to degenerative aortic valve disease; and 4) heart explants in the context of heart transplantation for ischemic or idiopathic dilated cardiomyopathy. These last valves were used for evaluating the presence of endothelial microfissuring. To avoid artifactual injury of the sample, the entire heart was explanted at a supravalvular level and transported immediately to our laboratory. After extensive washes in saline, the excision of the valve was carefully performed under microscope guidance. All aortic valves were immediately examined following tissue dissection, before any conditioning, and classified according to the degree of AC, including no calcification, microscopic calcifications, or macroscopic calcifications. Valves were thereafter washed in phosphate-buffered saline (PBS) and fixed by paraformaldehyde (PFA).

WHOLE-MOUNT ALIZARIN AND PERLS' BLUE STAINING OF VALVES. The proximity of calcium deposits with hematomas was visualized through the capacity of RBCs, the most abundant cells in the blood, to release iron, which was evaluated by Perls' staining, as described previously (8). After washing with distilled water, fixed valves were stained with Perls' blue solution freshly prepared from a mixture of 2.5% potassium ferrocyanide, 0.25% hydrochloric acid, and 0.02% Triton X-100 (Millipore Sigma, Merck, Darmstadt, Germany), for 90 min at room temperature. Valves were then washed with water and stained with freshly prepared 0.04% Alizarin red solution. After 1 h of incubation, the solution was discarded, samples were extensively washed with distilled water, and the tissue was clarified. The valve clarification method was adapted from the clearing procedure described by Yamazaki et al. (9). Briefly, valves were dehydrated successively in 25%, 50%, 75%, and 100% aqueous tetrahydrofuran solutions for 10 min and then for another 10 min in tetrahydrofuran and a freshly prepared solution of benzyl alcohol and benzyl benzoate at a ratio of 1:2 (BABB) (vol:vol). To increase valve transparency, tissues were placed in a BABB solution for 5 to 10 min. Valves were examined in 3 dimensions under a transmitted light microscope. Quantification of calcium and iron deposits was performed on all valves of the collection according to a 5-grade classification: grade 0 corresponded to the absence of both microscopic and macroscopic deposits; grade 1 corresponded to the presence of microscopic stains only (<5%); and grades 2, 3, 4, and 5 corresponded to the detection of macroscopic deposits of, respectively, <10%, <30%, <50%, and >75% of the valve surface.

WHOLE-MOUNT IMMUNOFLUORESCENCE STAINING.

We used whole-mount multiple immunofluorescence confocal microscopy (10) to distinguish VECs, VICs, and RBCs with lectin-rhodamine (Ulex Europaeus Agglutinin I, Vector Laboratories, Burlingame, California), anti-human alpha-smooth muscle actin (α SMA) (monoclonal, mouse, clone 1A4, Thermo Fisher Scientific, Waltham, Massachusetts), and anti-human glycophorin A (monoclonal, rabbit, Abcam, clone EPR8200) antibodies, respectively. Tissues were fixed in PFA, washed in water, and then dehydrated in methanol. After rehydration in TBST (50 mM Tris-HCl pH 7.4, 150 mM sodium chloride, 0.1% TritonX-100), tissues were incubated in a blocking solution containing 10% serum and then with primary antibodies and lectin-rhodamine diluted in blocking solution containing 5% dimethyl sulfoxide for 3 days. After extensive washing with TBST, incubation with secondary antibodies anti-mouse AF488 and anti-rabbit AF647 (Abcam, Cambridge, United Kingdom) was carried out using the same procedure. Images were taken by LSM 780 confocal microscopy (Zeiss, Oberkochen, Germany).

SCANNING ELECTRON MICROSCOPY. Valves were fixed in PFA, post-fixed in 2% glutaraldehyde, and dehydrated in graded ethanol solutions. Samples were air-dried at room temperature and mounted on aluminum stubs with double-stick tabs. Tissues were coated with 10 nm graphite, and imaging was performed under high-vacuum conditions at 10 or 20 kV using a Philips Quanta FEG 250 scanning microscope (Thermo Fisher Scientific).

VIC ISOLATION AND CULTURE. Primary human VICs were prepared as described previously (11) from noncalcified aortic valves obtained from explanted hearts of patients undergoing heart transplantation. The valve leaflets were excised and washed in PBS containing a 1% antibiotic mixture (penicillin, streptomycin, and fungicide). The leaflets were placed in a type I collagenase solution (0.22 U/mg) for 3 h at 37°C. After digestion, a cell suspension was obtained by removing undigested tissue pieces with a 70- μ m cell strainer. Cells were suspended in a complete smooth muscle cell basal 2 medium (PromoCell, Heidelberg, Germany) with 10% fetal bovine serum and a 1% antibiotic mixture (Thermo Fisher Scientific). VICs were seeded in tissue culture flasks in complete media and used for experiments or further subcultures until passage 4.

PREPARATION OF COLLAGEN SCAFFOLDS FOR 3-DIMENSIONAL VIC CULTURE AND STIMULATION. To mimic physiological conditions, VICs were cultured in 3-dimensional collagen scaffolds (12).

Fresh collagen solutions were prepared by mixing 0.3 ml of 10 \times concentrated DMEM (Dulbecco's modified Eagle's medium), 0.3 ml of 0.25 M sodium bicarbonate buffer, 0.3 ml of fetal bovine serum, 0.3 ml of antibiotic mixture, 0.12 ml of 0.1 M sodium hydroxide, and 2.5 ml of rat type I collagen (3 mg/ml, Gibco). After polymerization of the collagen mixture, primary cultured cells were seeded on collagen scaffolds at 30,000 to 50,000 cells/well and incubated for 2 days in complete medium before the addition of RBCs. Immunohistochemical staining and calcium deposits were analyzed in the cell cultures on days 5 and 7, respectively. Alizarin red (2%) was used to visualize calcium deposits.

IMMUNOHISTOCHEMISTRY. VICs were rinsed with PBS, fixed in PFA, washed with TBS (50mM Tris-HCl, 0.9% sodium chloride, 0.05% Tween 20 [Polysorbate 20], Merck, Darmstadt, Germany) and permeabilized with PBS, 0.05% Triton X-100 and 1% bovine serum albumin-glycine. Anti-human osteocalcin (monoclonal, mouse, clone 190125, R&D System, Minneapolis, Minnesota) and anti-human glycophorin A (GPA) (monoclonal, rabbit, Abcam, clone EPR8200) antibodies were incubated overnight and detected using the appropriate secondary antibodies (goat antimouse coupled to AF488 and antirabbit coupled to rhodamine). DAPI (4',6-diamidino-2-phenylindole, dihydrochloride) and AF647-coupled phalloidin (Life Technologies, Thermo Fisher Scientific) were used for counter staining. Slides were cover-mounted with Prolong Gold Antifade Reagent (Invitrogen, Thermo Fisher Scientific), and images were captured on an Axiovert 200 M inverted microscope (Zeiss, Göttingen, Germany).

RED BLOOD CELL PREPARATION. RBCs were prepared from human peripheral blood (13) collected from healthy volunteers in heparinized tubes. The pellet containing RBCs was mixed (1:1) with a dextran solution (2% in Hank's balanced salt solution [HBSS]) for 15 min, centrifuged and washed with HBSS. The resulting fresh RBCs (f-RBCs) served as controls. The senescence of RBCs from the same donor was induced by suspending f-RBC in HBSS supplemented with 0.1% glucose and incubated at 37°C for 5 days. The capacity of phosphatidylserine exposed on cell membranes to bind annexin-V-FITC (fluorescein isothiocyanate) was assessed by flow cytometry. Senescent RBCs (s-RBCs) were washed before in vitro assay to limit the direct effect of free hemoglobin.

GENE EXPRESSION. VICs were cultured for 24 or 48 h in the presence of f-RBC or s-RBC. Total RNA was extracted from cells using Trizol reagent (Invitrogen). Reverse transcription was performed on 20 ng of

TABLE 1 Human Primers Used for Quantitative Real-Time PCR

Gene	Forward	Reverse
HPRT	TGAGGATTGGAAAGGGTGT	GAGCACACAGAGGGCTACAA
IL6	GAAAGCAGCAAAGAGCCA	GTATACCTCAAACCTCAA
IL1 β	CGAATCTCCGACCACCACTA	GATCGTACAGGTGCATCGT
CBFA1	CCTCTGGCCTTCCACTCTCA	GACTGGCGGGGTGTAAGTAA
BSP	TCAGCATTTTGGGAATGG	TCTTCGGATGAGTCACTAC
OPG	GAAGCTGGAACCCAGAG	GTGTTCATTCTGAGTTA
RANK	AGGGAAAGCACTCACAGCTAA	ACATGCTCCCTGCTGACC
BMP2	AACGGACATTGGCTCTTGC	CCATGGTCGACCTTTAGGAGA
MSX2	CCTGTTGAGAGGAATTGATGG	AAAGGTATACCCGAGGGAGG

BMP2 = bone morphogenic protein 2; BSP = bone sialoprotein; CBFA1 = core-binding factor alpha 1; HPRT = hypoxanthine-guanine phosphoribosyltransferase; IL = interleukin; MSX2 = muscle segment homeobox 2; OPG = osteoprotegerin; PCR = polymerase chain reaction; RANK = receptor activator of nuclear factor kappa B.

total RNA with a Superscript III cDNA synthesis kit (Life Technologies) to obtain the cDNA target. Real-time polymerase chain reaction was performed on the CFX 100 (Bio-Rad, Hercules, California) cyclor using the primers listed in [Table 1](#). The reaction volume was performed with 1 ng of cDNA of each sample, 250 nM of forward and reverse primers and the Syber-Green master mix (Bio-Rad). The amplification program was performed as follows: 1 cycle: 50°C, 2 min; 1 cycle: 95°C, 15 min; 50 cycles: 95°C, 40 s, and 60°C, 1 min. The expression of the genes of interest was normalized by the expression of the housekeeping gene hypoxanthine-guanine phosphoribosyltransferase (*HPRT*) and the expression of VICs stimulated by f-RBC using the $2^{-\Delta\Delta CT}$ method (14).

PHAGOCYTOSIS ASSAY OF RED BLOOD CELLS. RBCs were labeled with Cell Tracker Violet (Thermo Fisher Scientific) and incubated with VICs. After 24 h or 48 h, unbound RBCs were removed by washing, and

cells were dissociated with trypsin. The cells were suspended in PFA and analyzed by flow cytometry (LSRII, BD Biosciences, San Jose, California).

STATISTICAL ANALYSIS. Variables were expressed as the mean \pm SD or number (percent). Distribution of variables was assessed using the Shapiro-Wilk normality test. Comparisons were performed using Student's *t*-test, the chi-square test, the Wilcoxon test, or the Fisher exact test as appropriate. A *p* value <0.05 was considered statistically significant. Statistical analyses were performed using JMP 10 software (SAS Institute, Cary, North Carolina).

RESULTS

AORTIC VALVE COLLECTION CHARACTERISTICS.

To obtain a global overview of the AC process, we collected aortic valves from patients with severe and moderate AS, as well as from patients free from any aortic valve disease. The valves were obtained from 40 (63%) patients with severe AS, 5 (8%) patients with moderate AS, 14 (22%) patients with pure aortic regurgitation, and 5 (8%) patients with healthy, calcium-free aortic valves from heart explants following heart transplantation. Baseline clinical and aortic valve characteristics in the overall study group and according to the degree of AC are reported in [Table 2](#). Briefly, the mean age of the patients was 66 ± 15 years, 43 (67%) were male, and the aortic valve mean pressure gradient was 42 ± 22 mm Hg. On the basis of Alizarin red staining, 11 (17%) valves were calcium free, 18 (28%) had microscopic calcifications, and 35 (55%) had macroscopic calcifications.

INTRALEAFLET HEMATOMAS, DETECTED BY IRON ACCUMULATION, PRECEDE CALCIUM DEPOSITION.

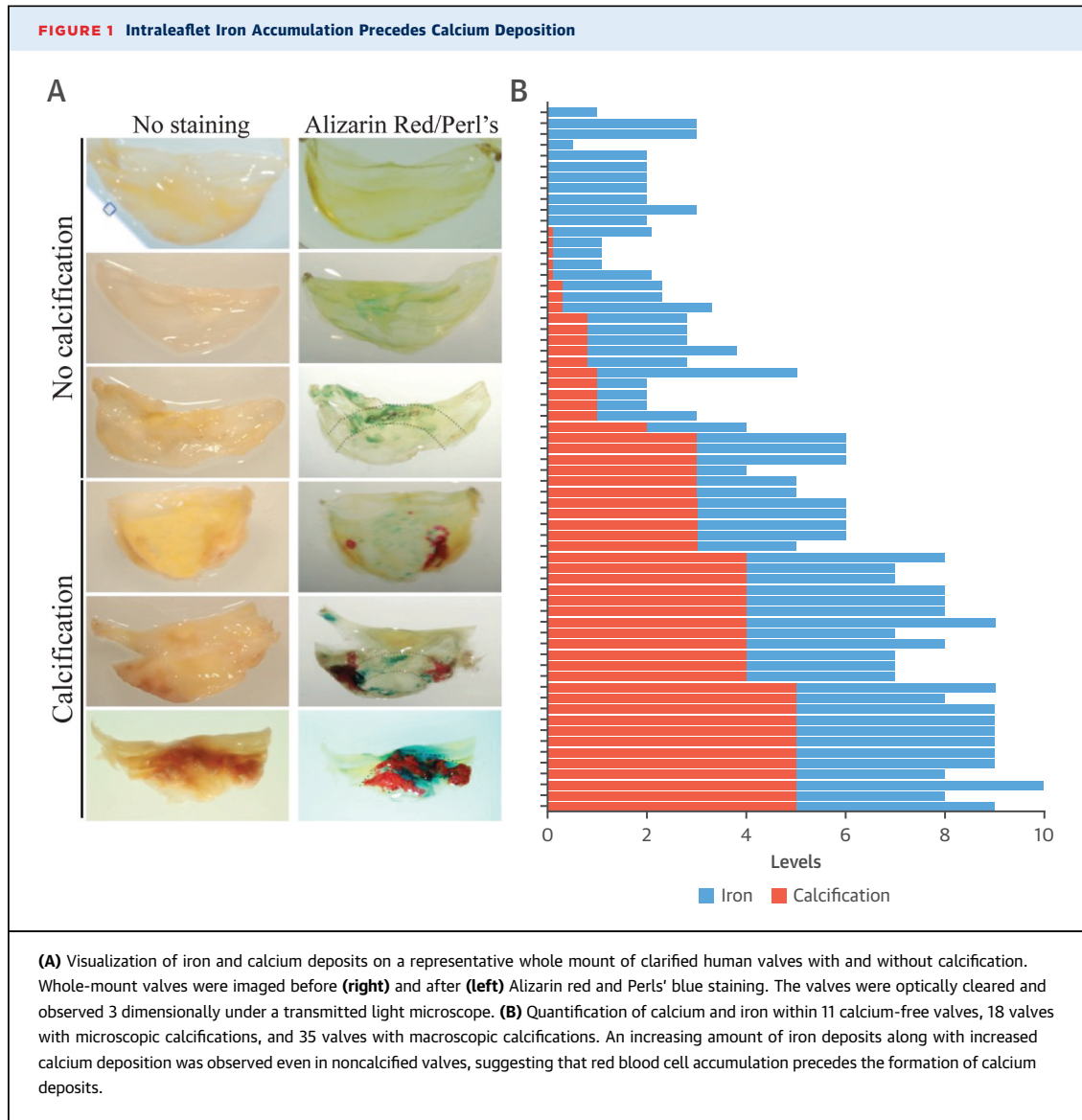
To establish a spatial link between calcium deposits and the areas of intraleaflet RBC accumulation, whole-mount examination of all aortic valves was performed after staining with Alizarin red and Perls' blue. An increasing amount of iron deposits was observed along with the increased calcium deposition within the valve, as shown in the representative image ([Figure 1A](#)), even in noncalcified valves, a finding suggesting that intraleaflet hematomas at the sites of valve calcification precede the formation of calcium deposits. The quantified results for all 64 valves are presented in [Figure 1B](#), thus confirming this observation.

Observation of valves with macroscopic calcifications collected from patients with severe AS revealed RBC accumulation in the immediate vicinity of the calcifications, mostly in areas adjacent to neoangiogenesis ([Figure 2A](#)). Examination of valve leaflets obtained from explanted hearts revealed the presence

TABLE 2 Baseline Clinical and Aortic Valve Characteristics in the Overall Population and According to Degree of Calcification

	Overall Population (N = 64)	No Calcification (n = 11)	Microscopic Calcification (n = 18)	Macroscopic Calcification (n = 35)	p Value
Age, yrs	66 \pm 15	47 \pm 12	70 \pm 15	72 \pm 9	<0.0001
Men	43 (67)	9 (82)	11 (61)	23 (66)	0.47
Coronary artery disease	18 (28)	2 (18)	6 (33)	10 (29)	0.66
Diabetes	14 (22)	2 (18)	3 (17)	9 (26)	0.71
Hypertension	28 (44)	3 (27)	7 (39)	18 (51)	0.33
Hypercholesterolemia	22 (34)	1 (9)	4 (22)	17 (49)	<0.02
Smoking	24 (38)	5 (46)	8 (44)	11 (31)	0.54
Anticoagulation therapy	12 (19)	4 (36)	4 (22)	4 (11)	0.17
Antiplatelet therapy	18 (29)	2 (18)	5 (28)	11 (31)	0.68
Mean pressure gradient, mm Hg	42 \pm 22	7 \pm 9	36 \pm 8	51 \pm 16	<0.008

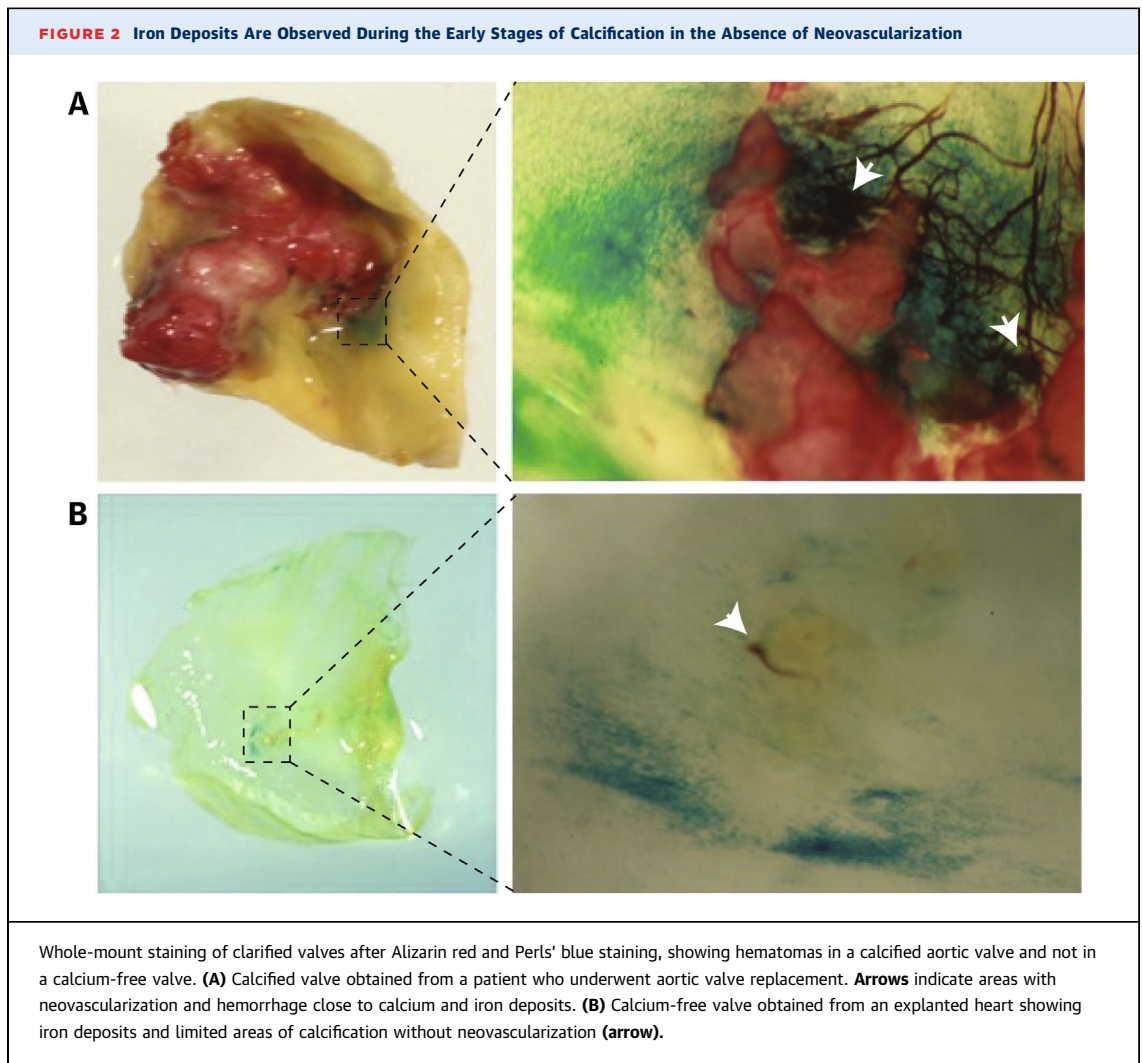
Values are mean \pm SD or n (%).



of iron deposits in the proximity of clusters of microcalcification but without associated neo-vascularization (Figure 2B). In light of these findings, we hypothesized that the iron deposits during the early stages of AC may be a consequence of the penetration of RBCs through VECs. Given that the endothelial layer is impermeable to RBCs under physiological conditions, these observations suggested that the observed intraleaflet hematomas could be secondary to local breaching of the endothelial barrier. The penetration of RBCs through breaches of the VEC layer could constitute the hematoma-forming mechanism dominating the early phase of AC, whereas hemorrhages through the leaky

intravalle neovessels, suggested by previous reports (6,7), likely constitute an additional source of hematomas during advanced stages of AC.

AORTIC VALVE ENDOTHELIUM INJURY IS ASSOCIATED WITH INTRALEAFLET RBC ACCUMULATION. To look for the presence of endothelial injury during the early stages of calcification, we analyzed the surface of the fibrosa side of the calcium-free valves by using scanning electron microscopy. We found areas of endothelial denudation in all valves, even in the absence of calcification (Figures 3C, 3E, and 3G). Within these areas, RBCs were entrapped in the matrix of the fibrosa (Figures 3D, 3F, and 3H). To



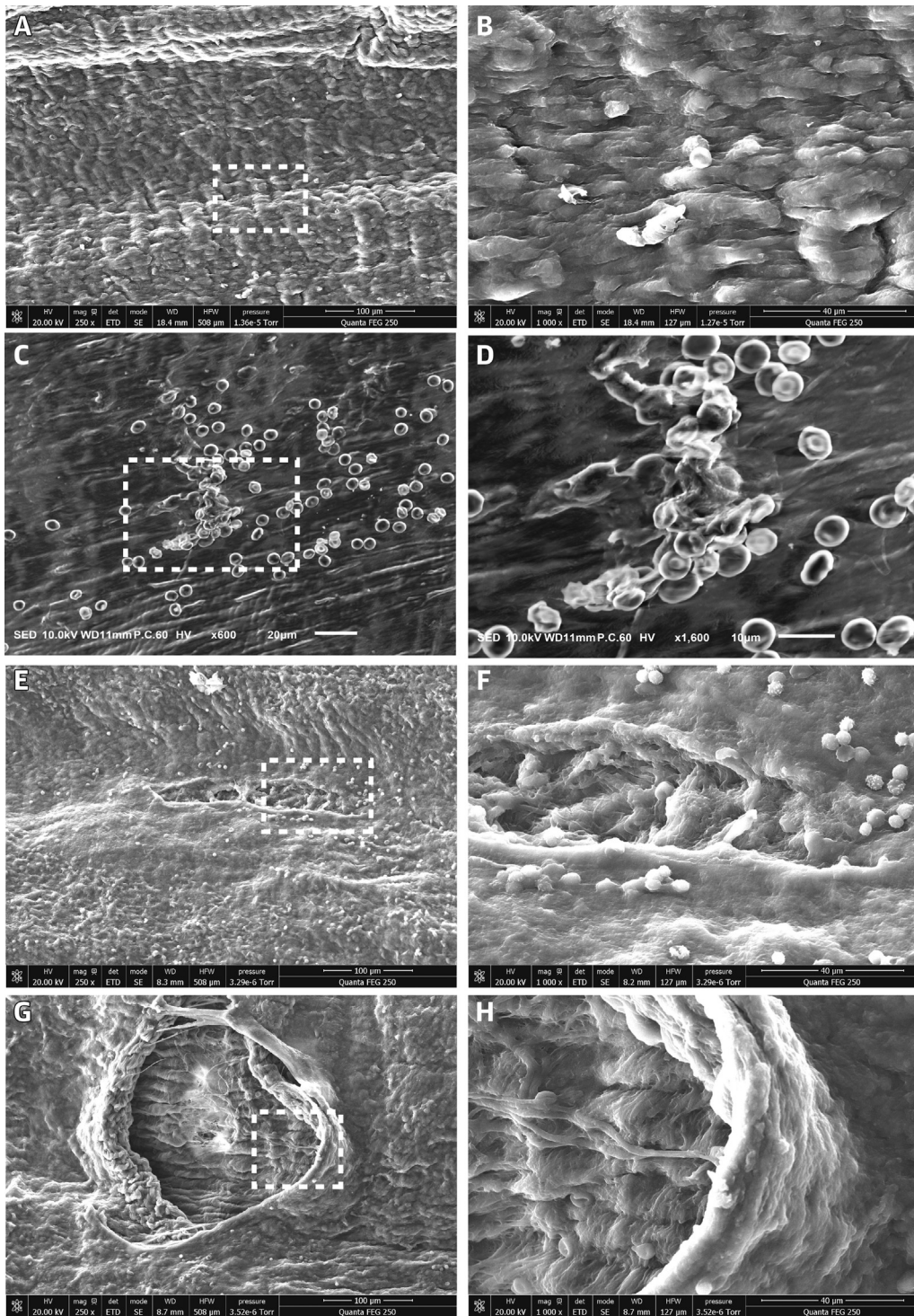
confirm these results, whole-mount immunostaining of VICs, VECs, and RBCs, with, respectively, anti- α SMA, anti-lectin and anti-glycophorin A (anti-GPA) antibodies, was performed on clarified aortic valves with microscopic calcifications and without neovascularization (Figure 4). Healthy areas contained VICs within the fibrosa covered by an unaltered endothelial barrier composed of VECs. In contrast, areas of endothelial denudation were characterized by a complete loss of VECs (Figures 4A and 4B). This loss of endothelium led to extensive penetration of RBCs into the fibrosa, as revealed by confocal Z-series images of whole-mount valves (Figure 4B). Quantification of the mean fluorescence intensity revealed a decrease in VEC density leading to contact between RBCs and VICs (Figure 4C). These results suggested that endothelial injury observed during early stages of calcification led to the deposition of iron that likely

was released from RBCs that had penetrated into the fibrosa.

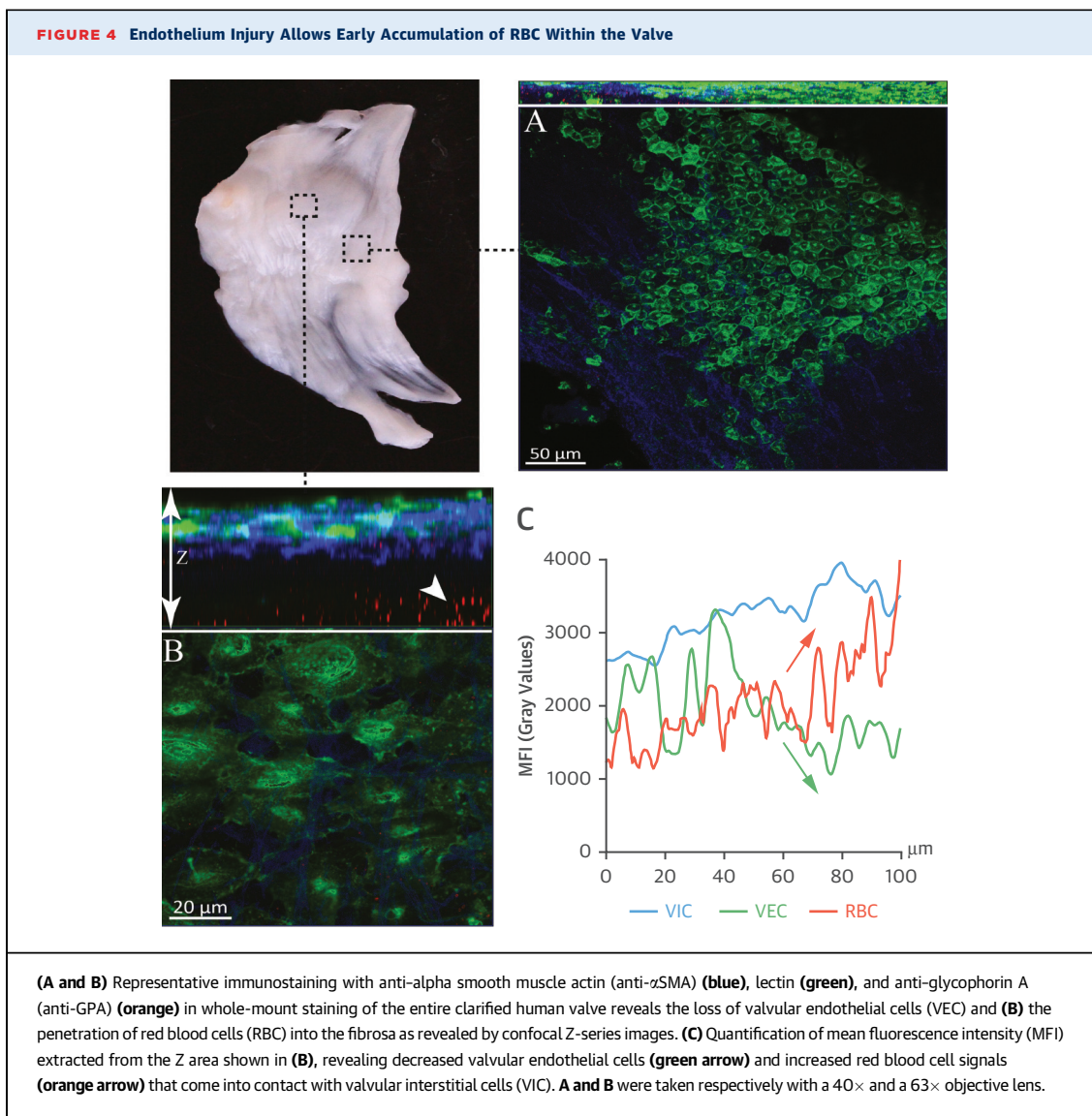
SENESCENT RBCs PROMOTE THE DIFFERENTIATION OF VICs TOWARD AN OSTEOLASTIC PHENOTYPE.

Valve injury causes the infiltration of blood and the contact of its elements with the cells of the fibrosa, which are not physiological condition. To mimic the biology of tissue-infiltrated blood in vitro, we used RBCs prepared from healthy donors. The absence of leukocytes in these blood preparations allowed us to use them with VICs derived from a different donor. Furthermore, considering that the RBCs undergo accelerated senescence after their accumulation in hematomas as a result of the static and pro-oxidative conditions (15,16), we prepared 2 types of RBC, s-RBCs and f-RBCs, to be used in our in vitro experiments with the VICs. We found that osteocalcin production and

FIGURE 3 Early Aortic Valve Endothelium Injury Leads to Intraleaflet RBC Accumulation



(A, C, E, G) Scanning electron microscope views of the fibrosa side of human aortic valves from explanted heart without calcification. **(A)** Area of the valve leaflet without endothelium injury. **(B)** Zoomed view of the boxed area presented in **(A)**. **(C, E, G)** Valve leaflet with endothelium denudation and penetration of red blood cells (RBCs) into the deeper layer of the fibrosa. **(D, F, H)** Zoomed view of the boxed areas presented, respectively, in **C, E, and G**.



calcium deposits were observed only when VICs were co-cultured with s-RBCs (**Figure 5A**). Furthermore, VICs were able to acquire inflammatory and pro-osteogenic profiles when they were co-cultured with s-RBCs for 24 or 48 h, as shown in **Figure 5B**. A statistically significant increase in the expression of interleukin (IL)-6, IL-1 β , bone sialoprotein, osteoprotegerin, the receptor activator of nuclear factor kappa B, bone morphogenic protein 2, and muscle segment homeobox 2 was noted.

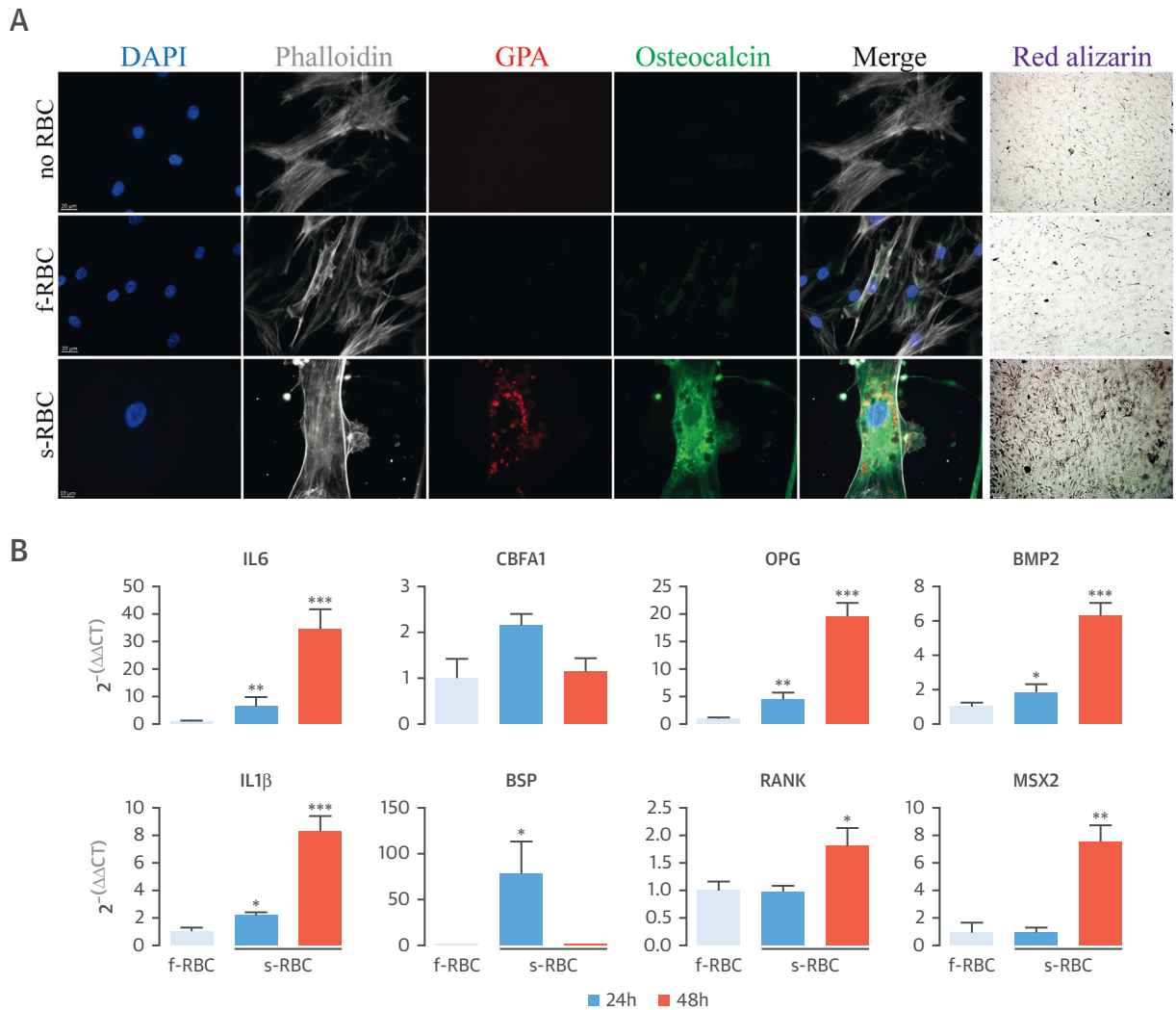
Incubation of s-RBCs on collagen scaffolds in the absence of VICs did not lead to calcium formation, thereby demonstrating the absolute requirement of VICs for calcification and excluding the possibility that an eventual interaction between the s-RBCs and the collagen scaffold could trigger calcification

(**Online Figure 1**). Interestingly, VICs were able to phagocytize s-RBCs, as shown by a representative orthogonal view using confocal microscopy (**Online Figure 2A**). This result was confirmed by flow cytometry, which showed an increased incorporation rate into the VICs of s-RBCs loaded with a violet cell tracer (**Online Figure 2B**).

DISCUSSION

The occurrence of intraleaflet hemorrhage has been suggested to accelerate the progression of human AC (**6,7**). These studies, however, exclusively focused on severely calcified valves at advanced disease stages. As a consequence, the etiopathogenic role of intraleaflet hematoma could not be evaluated.

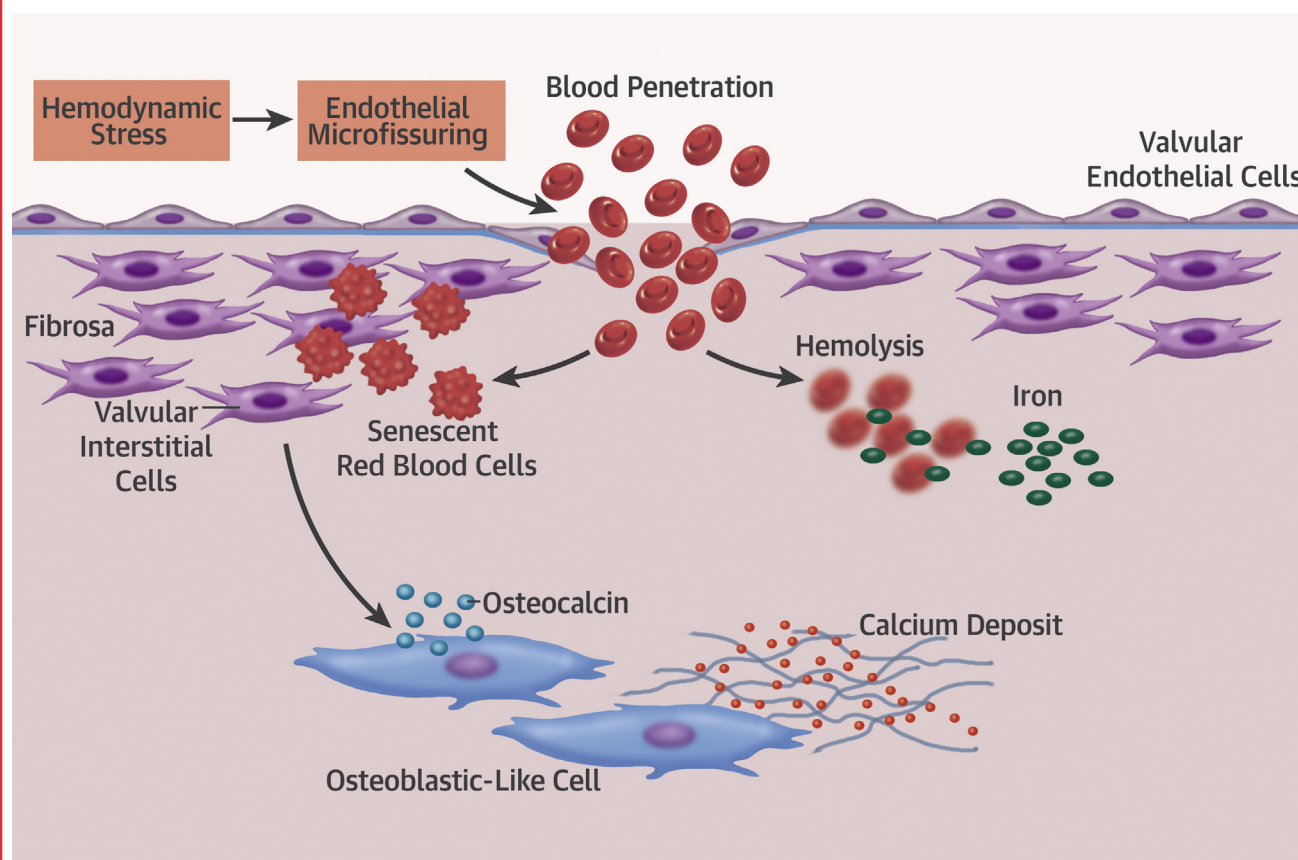
FIGURE 5 Senescent RBCs Promote VIC Differentiation Toward an Osteoblastic Profile In Vitro



(A) Human valvular interstitial cells (VIC) were cultured on a scaffold collagen in the absence (no red blood cells [RBC]) or presence of 2×10^6 of fresh red blood cells (f-RBC) or senescent red blood cells (s-RBC). At day 5, immunofluorescent staining of the nuclei (4',6-diamidino-2-phenylindole, dihydrochloride [DAPI]), the actin cytoskeleton (phalloidin), osteocalcin (anti-osteocalcin), and red blood cells (anti-glycophorin A [anti-GPA]) was performed in fixed cells. Cells cultured in the same condition were stained at day 7 by Alizarin red to visualize calcium deposits. **(B)** The expression levels of interleukin (IL)-6, IL-1 β , core-binding factor alpha 1 (CBFA1), bone sialoprotein (BSP), osteoprotegerin (OPG), receptor activator of nuclear factor kappa B (RANK), bone morphogenic protein 2 (BMP2) and muscle segment homeobox 2 (MSX2) were determined by reverse transcription-quantitative polymerase chain reaction on RNA extracted from valvular interstitial cells co-cultured with fresh or senescent red blood cells for 24 or 48 h. The gene expressions were determined by reverse transcription quantitative polymerase chain reaction and analyzed using the $2^{-\Delta\Delta Ct}$ Pfaffl formula (14), in which data were normalized to the expression of valvular interstitial cells stimulated with fresh red blood cells at 24 h and to the values of hypoxanthine-guanine phosphoribosyltransferase. Data are representative of four independent experiments. Results are presented as the mean \pm SEM and were analyzed with paired Student's *t*-tests: **p* < 0.05; ***p* < 0.01; ****p* < 0.0001.

In the present work, we analyzed a wide range of aortic valves in terms of calcification severity, including macroscopically and microscopically calcified valves representing early stages of the disease (Central Illustration).

Because the use of microscopic preparations does not allow for scanning for the presence of hematomas in the whole valve, we adopted a whole-mount method that allowed us to establish a precise spatial relationship between areas of hematoma and

CENTRAL ILLUSTRATION Intraleaflet Hematoma Promotes Aortic Valve Calcification

Morvan, M. et al. *J Am Coll Cardiol.* 2019;73(9):1043-54.

Blood penetration through an endothelial microfissure may drive the acquisition of an osteoblastic phenotype by valvular interstitial cells and determine the site of calcium deposition in human aortic valves. Endothelial microfissuring that occurs secondary to local hemodynamic stress allows red blood cells to penetrate into the fibrosa. The observation of free iron in "healthy valves" suggests that this could be the earliest trigger of the complex and chronic inflammatory process that leads to calcium deposition in aortic valves. In patients, the putative pathogenetic role played by such intraleaflet hematomas depends on the inability of valvular interstitial cells to cope with the entry of blood elements. Our *in vitro* data suggest that the initiation of calcium deposition in human aortic valves is driven by valvular interstitial cells that acquire an osteoblastic phenotype after coming into contact with infiltrated RBC displaying accelerated senescence and releasing free iron through red blood cell hemolysis.

calcification. We observed that hematomas detected by ferric iron deposits could be found not only in calcified valves, as previously shown, but also in noncalcified valves, a finding suggesting that intra-leaflet hematomas may precede, and possibly initiate, the development of AC.

Indeed, iron and calcium are co-localized in the proximity of areas exposed to increased mechanical stress (17), and several lines of evidence point at the specific hemodynamic stress experienced by the aortic valve at each closing cycle as a potential initiating factor that could lead to AC (18). The fibrosa of aortic valve leaflets has a singular structure with circumferentially oriented collagen fibers (18,19), and

during the diastolic phase of the cardiac cycle, it is exposed to significant hemodynamic forces and abrupt deformation (18). These hemodynamic and histological characteristics may contribute to the preferential occurrence of valve lesions within the fibrosa. We identified and quantified areas of endothelial denudation characterized by a complete loss of VECs and penetration of RBCs from the bloodstream into the fibrosa. This observation extends the previous paradigm by linking AC to intraleaflet hematomas not only caused by the rupture of fragile neovessels observed during late stages of the disease but also caused by the extrinsic penetration of arterial blood into the fibrosa as a consequence of microfissuring at

the earliest stages of AC. However, the microfissuring may not per se be considered a pathogenic trigger because all aortic valves are subjected to long-term mechanical stress. Thus, although the observed endothelial tearing may be considered an initiating event, other factors likely contribute to subsequent disease progression. In physiological conditions, the minor injuries that may occur recurrently at the surface of the fibrosa can be rapidly repaired by a highly coordinated series of events, including the activation of the blood clotting cascade, fibrin patch formation, and the inflammatory phase marked by the accumulation of neutrophils and macrophages, followed by a proliferative phase favoring tissue remodeling and reconstitution (20). In this sequence, the clearance of apoptotic cells, or efferocytosis, at the site of the lesion by macrophage engulfment constitutes a crucial step because the persistence of apoptotic cells can impede wound healing (21,22). Thus, accumulation of s-RBCs in areas of fibrosa microfissuring may witness a failure of the physiological efferocytosis, leading to a state of prolonged inflammation favoring the nonhealing of wounds. In such a situation, blood could continue to leak through the damaged endothelial wall, and the resulting expansion of the unresorbed hematoma could amplify the pathologic loop by prolonging the contact with the blood elements and driving the observed osteoblastic phenotypic changes of the VICs.

Differentiation of VICs toward an osteoblast-like phenotype is a well-described phenomenon (3,4,23,24), but the exact mechanisms and the nature of the endogenous factors that initiate these phenotypic changes still remain largely unknown. In healthy aortic valve leaflets, VICs are quiescent, with a fibroblast-like phenotype. In the present study, we found that VICs were able to acquire an osteoblast-like phenotype following contact with blood elements, particularly s-RBCs. The s-RBCs may act by releasing high amounts of iron, which may eventually drive the phenotypic changes of the stromal cells leading to the calcification process, as suggested by recent reports (25,26). Our observation, however also points at a novel function of the VICs, suggested by their ability to engulf intact RBCs. This observation suggests that besides macrophages, VICs could also contribute to the efferocytosis that is necessary to detoxify the valve microenvironment on the occurrence of an intraleaflet hematoma. VICs may therefore play a key role in the healing process of fibrosa injuries, thus contributing, under physiological conditions, to homeostasis of the aortic valve.

The contact of VICs with the elements of the bloodstream may represent a new pathophysiological

mechanism, which needs to be confirmed by future investigations, contributing to the initiation of AC. Interventions capable of preventing the extension of early intraleaflet hematomas and/or promoting their effective efferocytosis as well as physiological repair processes certainly represent a future axis of research to stop the progression of AC.

STUDY LIMITATIONS. The main limitation of our study is that the temporal sequence of the evolution of AC was not performed on the same individual. However, the longitudinal approach we adopted by studying a broad range of aortic valves at different stages of AC allowed us to comprehend the natural history of the disease.

CONCLUSIONS

Human AC is tightly linked to the penetration of blood elements into the valvular tissue. Injuries are likely to recur on valves because the valves are required to perform heavy mechanical work. Repair processes keep valves healthy, but concomitant noxious conditions can disturb the biology of resident cells and promote pathological conditions. Repeated aortic valve intraleaflet accumulation of s-RBCs after unhealed endothelial injury is such a noxious condition that may promote VIC differentiation toward an osteoblastic phenotype and favor calcium deposition leading to calcific AS.

ACKNOWLEDGMENT The authors greatly acknowledge Samira Benadda of the CRI U1149 Imaging Facility for her technical assistance.

ADDRESS FOR CORRESPONDENCE: Dr. Jamila Laschet, INSERM U 1148, Bichat Hospital, 46 rue Henri Huchard, 75018 Paris, France. E-mail: jamila.laschet@inserm.fr. Twitter: [@Inserm](https://twitter.com/Inserm). OR Dr. Giuseppina Caligiuri, INSERM U 1148, Bichat Hospital, 46 rue Henri Huchard, 75018 Paris, France. E-mail: giuseppina.caligiuri@inserm.fr.

PERSPECTIVES

COMPETENCY IN MEDICAL KNOWLEDGE: Iron released from erythrocytes that penetrate the fibrosa of human heart valves may be a consequence of endothelial injury during the early stages of calcification.

TRANSLATIONAL OUTLOOK: Further studies are needed to assess the potential therapeutic role of anti-inflammatory drugs that interfere with IL-1 β or IL-6 signaling in the progression of calcific AS.

REFERENCES

1. Baumgartner H, Falk V, Bax JJ, et al. 2017 ESC/EACTS guidelines for the management of valvular heart disease. *Eur Heart J* 2017;38:2739-91.
2. Nishimura RA, Otto CM, Bonow RO, et al. 2014 AHA/ACC guideline for the management of patients with valvular heart disease: a report of the American College of Cardiology/American Heart Association Task Force on Practice Guidelines. *J Am Coll Cardiol* 2014;63:e57-185.
3. Lindman BR, Clavel M-A, Mathieu P, et al. Calcific aortic stenosis. *Nat Rev Dis Primer* 2016;2:16006.
4. Pawade TA, Newby DE, Dweck MR. Calcification in aortic stenosis: the skeleton key. *J Am Coll Cardiol* 2015;66:561-77.
5. Yutzey KE, Demer LL, Body SC, et al. Calcific aortic valve disease: a consensus summary from the Alliance of Investigators on Calcific Aortic Valve Disease. *Arterioscler Thromb Vasc Biol* 2014;34:2387-93.
6. Akahori H, Tsujino T, Naito Y, et al. Intraleaflet haemorrhage is associated with rapid progression of degenerative aortic valve stenosis. *Eur Heart J* 2011;32:888-96.
7. Akahori H, Tsujino T, Naito Y, et al. Intraleaflet haemorrhage as a mechanism of rapid progression of stenosis in bicuspid aortic valve. *Int J Cardiol* 2013;167:514-8.
8. Asleh R, Guetta J, Kalet-Litman S, Miller-Lotan R, Levy AP. Haptoglobin genotype- and diabetes-dependent differences in iron-mediated oxidative stress in vitro and in vivo. *Circ Res* 2005;96:435-41.
9. Yamazaki Y, Yuguchi M, Kubota S, Isokawa K. Whole-mount bone and cartilage staining of chick embryos with minimal decalcification. *Biotech Histochem* 2011;86:351-8.
10. Alanentalo T, Asayesh A, Morrison H, et al. Tomographic molecular imaging and 3D quantification within adult mouse organs. *Nat Methods* 2007;4:31-3.
11. Chen J-H, Yip CYY, Sone ED, Simmons CA. Identification and characterization of aortic valve mesenchymal progenitor cells with robust osteogenic calcification potential. *Am J Pathol* 2009;174:1109-19.
12. Bellows CG, Melcher AH, Aubin JE. Contraction and organization of collagen gels by cells cultured from periodontal ligament, gingiva and bone suggest functional differences between cell types. *J Cell Sci* 1981;50:299-314.
13. Kolb S, Vranckx R, Huisse M-G, Michel J-B, Meilhac O. The phosphatidylserine receptor mediates phagocytosis by vascular smooth muscle cells. *J Pathol* 2007;212:249-59.
14. Pfaffl MW. A new mathematical model for relative quantification in real-time RT-PCR. *Nucleic Acids Res* 2001;29:e45.
15. Minetti M, Agati L, Malorni W. The microenvironment can shift erythrocytes from a friendly to a harmful behavior: pathogenetic implications for vascular diseases. *Cardiovasc Res* 2007;75:21-8.
16. Comporti M, Signorini C, Buonocore G, Ciccoli L. Iron release, oxidative stress and erythrocyte ageing. *Free Radic Biol Med* 2002;32:568-76.
17. Thubrikar MJ, Aouad J, Nolan SP. Patterns of calcific deposits in operatively excised stenotic or purely regurgitant aortic valves and their relation to mechanical stress. *Am J Cardiol* 1986;58:304-8.
18. Bäck M, Gasser TC, Michel J-B, Caligiuri G. Biomechanical factors in the biology of aortic wall and aortic valve diseases. *Cardiovasc Res* 2013;99:232-41.
19. Stella JA, Sacks MS. On the biaxial mechanical properties of the layers of the aortic valve leaflet. *J Biomech Eng* 2007;129:757-66.
20. Eming SA, Krieg T, Davidson JM. Inflammation in wound repair: molecular and cellular mechanisms. *J Invest Dermatol* 2007;127:514-25.
21. Gurtner GC, Werner S, Barrandon Y, Longaker MT. Wound repair and regeneration. *Nature* 2008;453:314-21.
22. Jun J-I, Kim K-H, Lau LF. The matricellular protein CCN1 mediates neutrophil efferocytosis in cutaneous wound healing. *Nat Commun* 2015;6:7386.
23. Mohler ER, Gannon F, Reynolds C, Zimmerman R, Keane MG, Kaplan FS. Bone formation and inflammation in cardiac valves. *Circulation* 2001;103:1522-8.
24. Rajamannan NM, Evans FJ, Aikawa E, et al. Calcific aortic valve disease: not simply a degenerative process: a review and agenda for research from the National Heart and Lung and Blood Institute Aortic Stenosis Working Group. Executive summary: calcific aortic valve disease-2011 update. *Circulation* 2011;124:1783-91.
25. Laguna-Fernandez A, Carracedo M, Jeanson G, et al. Iron alters valvular interstitial cell function and is associated with calcification in aortic stenosis. *Eur Heart J* 2016;37:3532-5.
26. Kawada S, Nagasawa Y, Kawabe M, et al. Iron-induced calcification in human aortic vascular smooth muscle cells through interleukin-24 (IL-24), with/without TNF-alpha. *Sci Rep* 2018;8:658.

KEY WORDS aortic valve stenosis, calcification, endothelium, hematoma, iron

APPENDIX For supplemental figures, please see the online version of this paper.